25th ABCM International Congress of Mechanical Engineering
October 20-25, 2019, Uberlândia, MG, Brazil

COB-2019-0223
NUMERICAL STUDY OF FLOW OVER SINGLE CYLINDERS: A FIXED CYLINDER AND A CYLINDER FREE TO VIBRATE

Roberta Fátima Neumeister
Adriane Prisco Petry
Sergio Viçosa Möller
Universidade Federal do Rio Grande do Sul, Porto Alegre, Brazil
e-mails: roberta.neumeister@ufrgs.br; adriane@mecanica.ufrgs.br; svmoller@ufrgs.br

Abstract. *The purpose of this paper is to present the main characteristics on a flow over a fixed single cylinder and a single cylinder free to vibrate to observe the main changes generated by freedom to vibrate. The vibration amplitude and dominant frequencies are also studied with changes in the reduced velocity and natural frequency. The two-dimensional and three-dimensional simulations are executed in ANSYS Fluent 18 using URANS (Unsteady Reynolds Averaged Navier Stokes) with turbulent model kω-SST. For the simulations with freedom to vibrate the moving mesh is applied. The tested Reynolds number ranges between 213 and 21.3x10^3 and the reduced velocity changed between 0.62 and 166. Fixed cylinder and free to vibrate cylinder present variations in the amplitude of the vortex street. The results present the non-dimensional amplitude, the power spectrum and vortex shedding pattern for the tested cases and show that the changes in the patterns of vortex shedding are linked to the increase in the vibration amplitude. The power spectrum showed frequencies agreeing with the natural frequency and the vortex shedding frequency. The results of pressure field show a region of influence around the cylinder higher than in the cylinder free to vibrate.*

Keywords: *Fixed Cylinder, Free to vibrate cylinder, Numerical Simulation.*

NOMENCLATURE

U	Velocity	[m/s]	D	Diameter	[D]
ν	Cinematic Viscosity	[m²/s]	m	Mass	[kg]
K	Stiffness	[N/m]	fs	Shedding Frequency	[Hz]
fn	Natural Frequency, $fn = \frac{1}{2\pi}\sqrt{\frac{K}{m}}$	[Hz]	S	Strouhal Number, $S = \frac{fs\,D}{U}$	[-]
Vr	Reduced Velocity, $Vr = \frac{U}{fn\,D}$	[-]	f*	Frequency ratio, $f^* = \frac{fs}{fn}$	[-]
Re	Reynolds Number, $Re = \frac{UD}{\nu}$	[-]			

1. INTRODUCTION

The flow over cylinders is applied in many engineering analyses, as tube banks and transmission lines. In some of these applications, the cylinders are fixed but, in many cases, the cylinders present freedom to vibrate in one or more directions. The characteristics of the flow, as the vortex formation, change when the cylinder is free to vibrate as presented by Blevins (1990), Govardhan and Williamson (2004) and Dong and Karniadakis (2005). To understand the influence of the cylinder vibration in the flow is important to study fixed cylinders in the same external conditions.

Studies that explore the vortex shedding mechanisms and tools for analysis of the flow on fixed bluff bodies using variations of influence parameters are presented in Zdravkovich (1997) and show the most relevant characteristics. The study of Möller et al., 2015, presented an experimental study, using hot wire anemometry for measurements on the wake of a positioned cylinder, in an aerodynamic channel with focus on the vortex shedding. The studies were performed using wavelets transform and Fourier transform. The results showed that the vortex shedding is not constant over time. A comparison with a prism indicates distinct behaviors in both cases. A correlation for Strouhal number correction as a function of the blockade ratio was presented.

Navrose, 2017, executed the two-dimensional numerical analysis of multiple responses of induced vibration in cylinders for Reynolds number 100, changes in the mass ratio and initial conditions were executed. The author

presented the main characteristics of amplitude and lift coefficient for a range of reduced velocity between 4.3 and 9, showing regions of higher and lower amplitudes, including regions out of the expected range, the response presented influence of the accelerating or deaccelerating flow. The mass ratio was varied from 10 to 150 and presented multiple regime states.

Wang et al., 2017 presented an experimental study of flow over cylinder free to vibrate using PIV to characterize the flow patterns changing the Reynolds Number and reduced velocity. The authors presented the increase in the amplitude and showed the change of vortex shedding pattern from two single vortex (2S) for two pairs of vortices (2S).

Jung et al., 2018, evaluated the wake of a flow behind a finite flexible cylinder and compared to the flow behind a rigid cylinder using flow visualization, particle image velocimetry, and modal orthogonal decomposition analysis. Spectral analysis demonstrates that the oscillatory motion of a flexible cylinder strongly influences the flow behind the cylinder. The flows behind the rigid and flexible cylinders are different near the free end of the cylinder. The downward flow of the free end of the flexible cylinder is relatively weak compared to the rigid cylinder. Behind the tip of the flexible cylinder, large-scale vortices are eliminated and propagated downstream, but these phenomena are not observed behind the rigid cylinder.

Gsell et al., 2018, studied numerically, applying direct numerical analysis, the three-dimensional structure of the flow downstream of a circular cylinder, considering fixed cylinder and subjected to vortex-induced vibrations. The Reynolds number applied was 3900, based on the cylinder diameter and free flow velocity. The flow was characterized by undulations of the shear layers that separate from the body and the development of planar vortices. The flow structure presented changes to the vibrating cylinder. In the region of the shear layer, body motion was associated with increased planar vortex formation.

The flow presents, in all circumstances, three-dimensional characteristics, but in some cases two-dimensional studies can be performed to understand some behaviors and better define three-dimensional studies. The present study aims to identify the flow main structures for one fixed cylinder and a cylinder free to vibrate in the same initial flow conditions. Investigate the transversal vibration amplitude of a cylinder with flow velocity changes for two-dimensional and three-dimensional simulation cases. The changes in the vibration amplitude and the flow characteristics with the reduced velocity change are also explored.

2. METHODOLOGY

The numerical analysis solves the Navier-Stokes equations applying Reynolds decomposition, the equations represent the continuity and the momentum (Tennekes and Lumley, 1972 and Wilcox, 2000). The solutions of the Navier-Stokes equations, with the Reynolds decomposition creates the problem of closure, since there are more unknowns than equations for solution. The turbulence models solve this impasse using the Boussinesq approach, which considers a turbulent viscosity presented in Wilcox (2000).

The equations Unsteady Reynolds Average Navier-Stokes (URANS) are solved using the turbulence model kω - SST (Shear Stress Transport). The application of the model kω - SST is recommended for flows with adverse pressure gradient. The shear stress transport model (SST) was developed to mix the kω model formulation in the near wall region with the independence of the kε model in the distant field of the wall. To achieve this, the kε model is converted into the kω formulation. The SST model is similar to the standard kω model, but includes some refinements, as different constants. The equations applied to obtain each term of the model are detailed in ANSYS (2018).

To study the cylinder moving in one direction, the degrees of freedom and dynamic mesh were applied. According to ANSYS, 2018, the dynamic mesh model allows moving the boundaries of a cell zone relative to other zone boundaries. The movement of the boundaries can be rigid or deforming, in both cases, the nodes that define the cells in the domain must be updated as a function of time, and therefore the dynamic mesh solutions are transient. The dynamic mesh model can be used to model flows where the shape of the domain is changing over time due to movement within the boundaries of the domain. The generic transport equation applies to all equations such as turbulence, energy, species and phases. The motion is determined based on the solution at the present time, from the balance of force in a solid body and the volume mesh refresh at each time step based on the new boundary position (ANSYS, 2018).

The tested domain present dimensions of 146x193x680 mm, for the two-dimensional analysis the dimension of 146mm was not accounted. The cylinder present diameter of 32mm and is positioned 150mm from the inlet and centralized in the width, the numerical domain is presented in Figure 1.

The mesh is constructed using tetrahedral volumes with prismatic layer in the cylinder and in the sides wall. The y+ in all meshes is under 5. The cases with freedom to vibrate are simulated with dynamic mesh, where the same rigid mesh is applied but allow the movement of the cylinder, due the flow forces and deformation is observed in the mesh. The deformation zone is presented in Figure 1 and outside the indicated region; the mesh does not move and represent a limitation in the amplitude of vibration.

The present study tested cases generating Reynolds number between 213 and $21.3x10^3$. The two-dimensional mesh quality was analyzed applying the GCI method (Grid Convergence Index) proposed by Roache (1994) and detailed in Roache (1997). The GCI indicates the error range that the solution is from the asymptotic value. The GCI is calculated for the mesh combinations, coarse-medium and medium-refined, the three meshes of size 114,768 volumes, 228,352

volumes and 457,888 volumes, the GCI was applied with the mean pressure coefficient on the cylinder. The convergence order value results in 1.2 and the relation between the GCIs from the finer mesh and coarser mesh generate a relation between GCIs of 0.945, indicating that the mesh is in the asymptotic region. The option is the use of the medium mesh with 228,352 volumes. The three-dimensional analysis was executed in a tetrahedral mesh with 3,287 thousand volumes and the y+ remained under 5, but no mesh independence study was executed.

The boundary conditions considered in all simulations are prescribed velocity in the inlet with length scale of 0.001 m and turbulence intensity of 0.6 %. The channel sides and the cylinder are considered no slip wall. The outlet is considered as atmospheric pressure. The time step used in the simulation is of 0.001s.

The two-dimensional analysis for a fixed cylinder are executed for three velocities and the cases generate Reynolds Number from 213 to 6400. The cases are identified with the prefix F and the main information about the fixed cylinder simulations are listed in Table 1.

Figure 1. Numerical domain and boundary conditions.

Table 1. Simulated cases with fixed cylinder.

Identification	Simulation	Velocity [m/s]	Diameter [mm]	Reynolds Number
F01	Two-Dimensional	0.1	32	213
F02	Two-Dimensional	0.8	32	1706
F03	Two-Dimensional	3	32	6400

The simulations for the cylinder free to vibrate were performed with mass 0.1kg, freedom to vibrate transverse to the flow and spring constant of 14N/m and 100N/m. These characteristics generate a natural frequency without damping of 1.88 Hz and 5.03Hz, the natural frequency is calculated relating stiffness and mass as described in Kelly (2000). The air flow velocity prescribed was changed from 0.1 m/s to 10 m/s. The simulations with freedom to vibrate are identified with the prefix V and the main characteristics are listed in Table 2 with the flow velocity, natural frequency, reduced velocity and Reynolds Number.

Table 2. Simulated cases with cylinder free to vibrate.

Case	Simulation	Velocity [m/s], U	Diameter [m], D	Reynolds Number, Re	Mass [kg], m	Stiffness [N/m], K	Natural Frequency [Hz], fn	Reduced Velocity, Vr
V01	Two-Dimensional	0.1	32	213	0.1	100	5.03	0.62
V02	Two-Dimensional	0.8	32	1706	0.1	100	5.03	4.97
V03	Two-Dimensional	3	32	6400	0.1	100	5.03	18.63
V04	Two-Dimensional	0.1	32	213	0.1	14	1.88	1.66
V05	Two-Dimensional	0.3	32	640	0.1	14	1.88	4.98
V06	Two-Dimensional	0.5	32	1066	0.1	14	1.88	8.3
V07	Two-Dimensional	5	32	10066	0.1	14	1.88	83.11
V08	Two-Dimensional	6	32	12800	0.1	14	1.88	99.73
V09	Two-Dimensional	8	32	17066	0.1	14	1.88	132.66
V10	Two-Dimensional	10	32	21333	0.1	14	1.88	166.22
V11	Three-Dimensional	0.2	32	426	0.1	14	1.88	3.32
V12	Three-Dimensional	3	32	6400	0.1	14	1.88	49.86

The cases with cylinder free to vibrate are tested for velocities that generate shedding frequency equivalent to the natural frequency of the cylinder, and with velocity higher and lower. The shedding frequency was estimated applying de Strouhal number equal to 0.2. This condition was used because when the natural frequency and shedding frequency synchronize higher amplitudes are expected.

The reduced velocity, Vr, is a non-dimensional relation used for indicating the flow velocity using the natural frequency and the cylinder diameter. The tested cases generate reduced velocity between 0.62 up to 166. The analyses of the simulations are executed with the amplitude of vibration history, Fast Fourier Transform in the signals from the simulations as described in Tennekes and Lumley (1972), pressure and velocity fields to evaluate the main structures in the flow.

3. RESULTS AND DISCUSSIONS

The results present the comparison between the main flow characteristics for fixed and free to vibrate two-dimensional analysis. The pattern with the increase of velocity and predominant frequencies in the two-dimensional analysis are also discussed. Some three-dimensional results are presented.

3.1 Flow pattern for fixed and free to vibrate cylinder

The flow pattern and wake formation change due the freedom to vibrate and these changes were investigated with simulations for fixed cylinders in the cases F01, F02 and F03, detailed in Figure 2. The pressure fields and velocity fields are observed in Figure 2 A to F, and the main change are the magnitude of pressure/velocity and the space between the vortex in the wake. The frequency of vortex detachment is the main change between F01, F02 and F03, as expected.

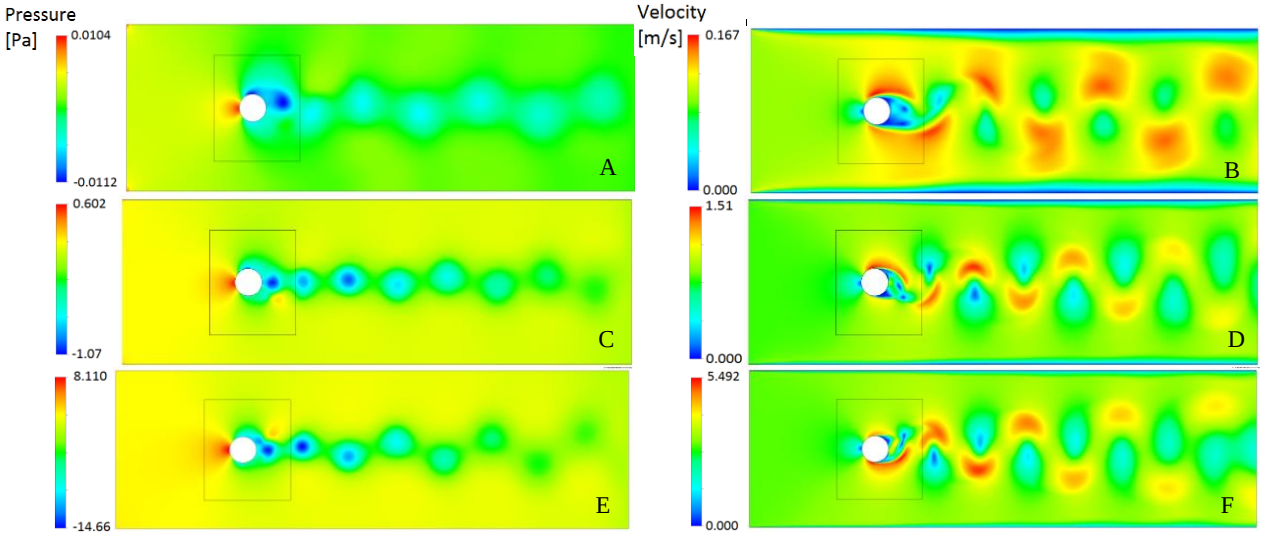

Figure 2 –Results with simulation time over 4s for A) Pressure field of Fixed cylinder Case F01, B) Velocity field of Fixed cylinder Case F01, C) Pressure field of Fixed cylinder Case F02, D) Velocity field of Fixed cylinder Case F02, E) Pressure field of Fixed cylinder Case F03 and F) Velocity field of Fixed cylinder Case F03.

The pattern for the cylinder free to vibrate were investigated with simulations in the cases V01, V02 and V03, detailed in Figure 3, where the initial conditions of the flow were equivalent with the fixed cases, but with freedom to vibrate on imposed natural frequency and the pressure and velocity fields are observed in Figure 3 A to F.

The results for the cylinder free to vibrate present inclination in the pressure field before the cylinder, as can be noticed in Figure 3 E in comparison with Figure 2E, this is linked to the movement in the cylinder caused by the resultant force on the rigid body.

In the velocity fields for fixed cylinder the regions in the cylinder sides present higher velocities, as can be observed in Figure 2 D and F. The cylinder free to vibrate, Figure 3 D and F. This change in the velocity magnitude can be linked to the influence of the fixed body in Figure 2, while in the moving body the energy changed the cylinder position, even in the cases where the low amplitude is observed.

Zdravkovich (1997) listed that streamwise oscillations is one of the typical disturbances on the flow among others as aspect ratio, roughness, blockage ratio, free end and boundary. The present comparison shows the same two-dimensional domain, Reynolds Number and blockage ratio, the changed characteristic is the cylinder free to vibrate in the transversal direction. For both cases, fixed and free to vibrate, the inlet velocity is 0.8m/s, Re = 1400, the Reynolds

Number characterizes the flow as subcritical state and for the case free to vibrate generates a shedding frequency around the natural frequency of the cylinder, that is estimated in 5.08Hz.

The results of velocity and pressure in the domain for the fixed cylinder, F02, were presented in Figure 3 C and D, in Figure 4 the results are presented with change of 3s in the simulation to represent the evolution in time. The results show the wake region developed with changes in the detaching position, but with most of the characteristics remaining equivalent.

The results for the cylinder free to vibrate, V02, were presented in Figure 3 C and D for time 5s and are presented with time evolution in Figure 5 with three frames spaced 3s during the simulation. In 4s, Figure 5 A and B, and 7s, Figure 5 C and D, is observed increase in the pressure around the cylinder but with the main characteristics remaining similar, in 10s, Figure 5 E and F, the pressure field present a significant change in the pressure distribution, with change in the shedding pattern. The velocity field shows the change of vortex characteristics, the variation in the cylinder position is also clear in 10s, while between 4s and 7s the position present small changes. Govardhan and Williamson (2004) and Wang et al. (2017) presented the observed change in the shedding pattern. The authors showed two single vortices formed per cycle, called 2S, as observed in 4s and 7s, the pattern in 10s is called 2P, two pairs of vortices formed by cycle, mainly visible in the pressure fields. The authors showed the patterns as characteristics of the flow for mass ratio and reduced velocity, but not as an evolution of the flow as observed. Navrose (2017) present characteristics of vibration for low Re and showed results with the variation of amplitude along time, as observed in Figure 5F.

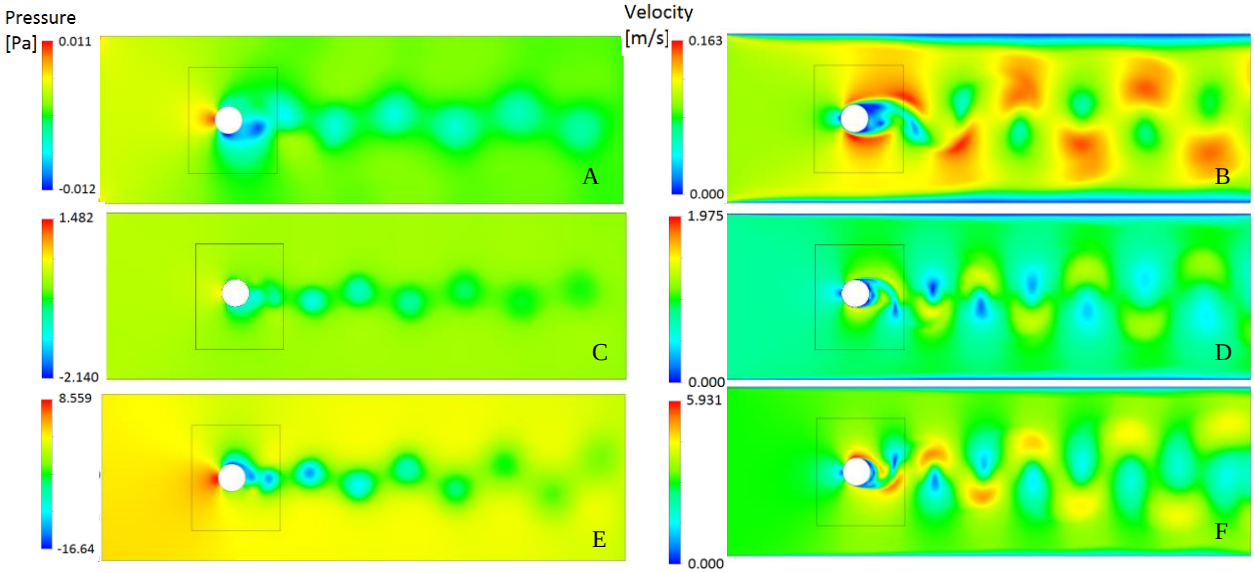

Figure 3 – Results with simulation time over 4s for A) Pressure field of Free to vibrate cylinder Case V01, B) Velocity field of Free to vibrate cylinder Case V01, C) Pressure field of Free to vibrate cylinder Case V02, D) Velocity field of Free to vibrate cylinder Case V02, E) Pressure field of Free to vibrate cylinder Case V03 and F) Velocity field of Free to vibrate cylinder Case V03.

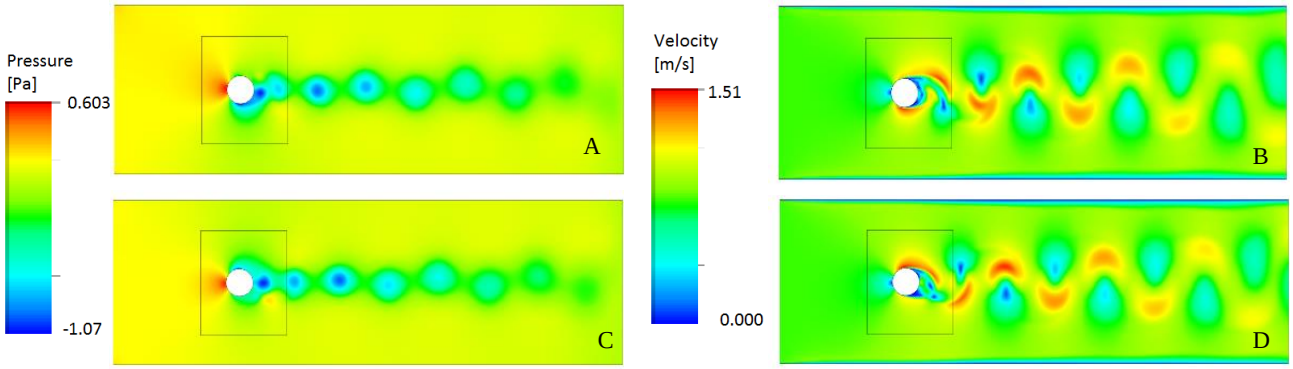

Figure 4 – Results for the case F02 with A) Pressure field in 5s, B) Velocity field in 5s, C) Pressure field in 8s and D) Velocity field in 8s.

The results of drag and lift for the compared cases F02 and V02 were also evaluated and are presented in Figure 6. The Figure 6 a) presents the drag and lift coefficients from the simulation F02 with the main changes under 1s, but after that the history remain with the same mean value. The Figure 6 b) presents the drag and lift coefficients from the simulation V02 with changes under 1s and again after 6s. The main changes observed are related to the drag coefficient that present higher oscilation in the case free to vibrate in relation to the fixed cylinder. After 6s the lift coefficient starts to also oscillates and around 8s presents a beating characteristic, presenting low values of drag and lifts coefficient. This behavior coincides with the change in the vortex shedding pattern from 2S (two single vortices) to 2P (two pairs of vortices), observed in Figure 5. The change of shedding pattern influences the lift and drag forces as can be observed after 8s in Figure 6 b), Navrose (2017) showed the relation between lift coefficient and vibration amplitudes change depending on the region of reduced velocity and in some cases the change in the pattern is observed.

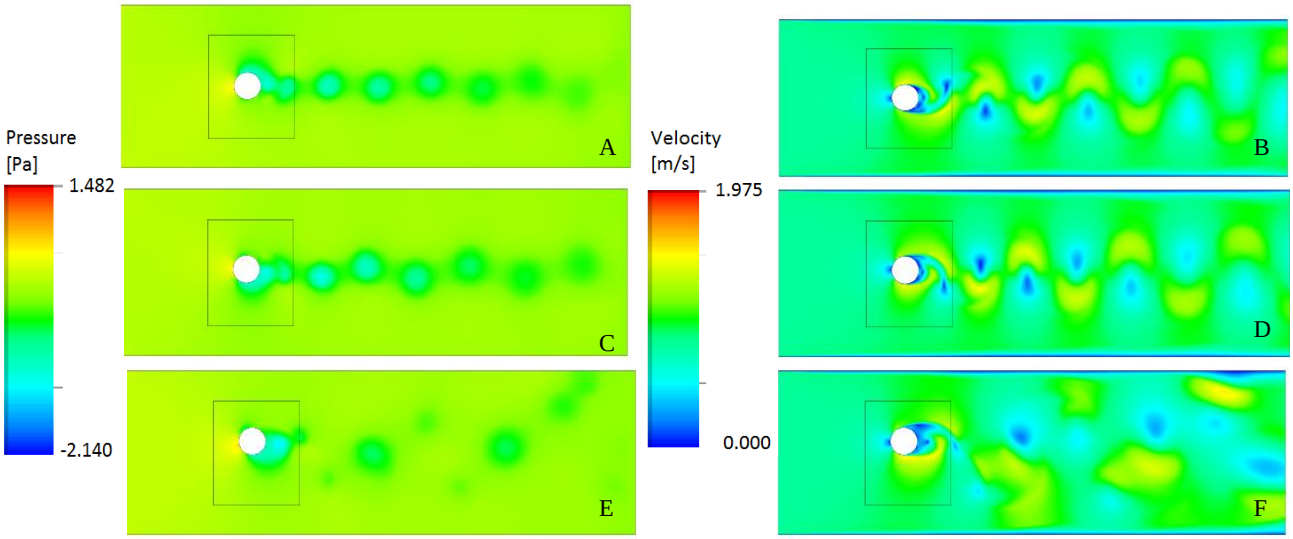

Figure 5 – Results for the case V02 with A) Pressure field in 4s, B) Velocity field in 4s, C) Pressure field in 7s, D) Velocity field in 7s, E) Pressure field in 10s and F) Velocity field in 10s.

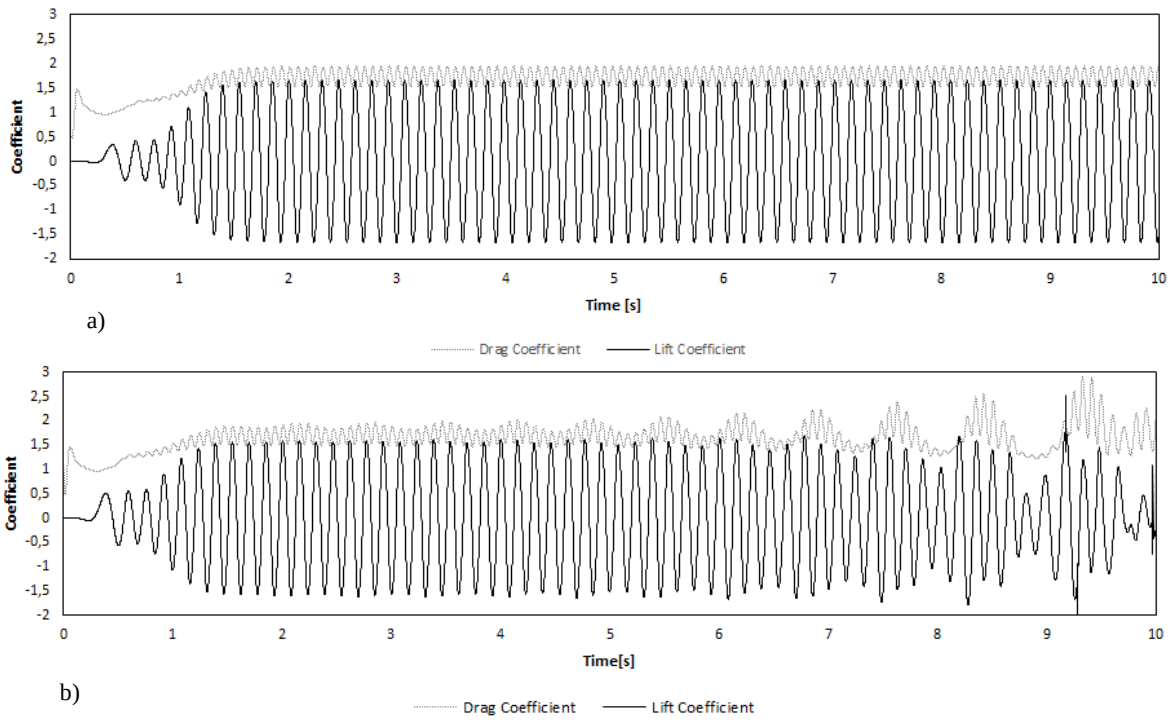

Figure 6 – Drag and lift coefficient a) Fixed and b) free to vibrate

3.2 Amplitude and Frequencie Results – Two-dimensional

The two-dimensional simulations to observe the response of the cylinder in a large range of reduced velocity were performed for at least 10s and the cylinder vibration history for Case V01 to V10, as described in Table 2, are presented in Figure 7. The non-dimensional amplitude Y/D is calculated with the rms mean amplitude Y from the vibration history and D is the cylinder diameter, the results in Figure 7 are separated by the tested natural frequencies. The Figure 7b) present the frequency ratio for the tested cases and showing that remain with crescent linear relation for f* higher than 1. For the region around 1 the relation remain around 1 as can be observed in Figure 7c).

The amplitude Y was obtained with mean value after 4s of simulation, to avoid the initial behavior as observed in Figure 8 a). The results show in all cases low amplitudes and even for the higher magnitudes around reduced velocity of 5, this can be associated with the use of air with work fluid and low density of the fluid. The natural frequency change from 1.88Hz to 5.08Hz show a significant change in the non-dimensional amplitude and can be linked to the proximity of the vortex shedding frequency, because the additional cases with fn 1.88Hz present similar non-dimensional amplitudes. The vibration response, frequency spectrum and pressure field are presented for the cases V09, V06, V05 and V02 from Figure 8 to Figure 11, respectively

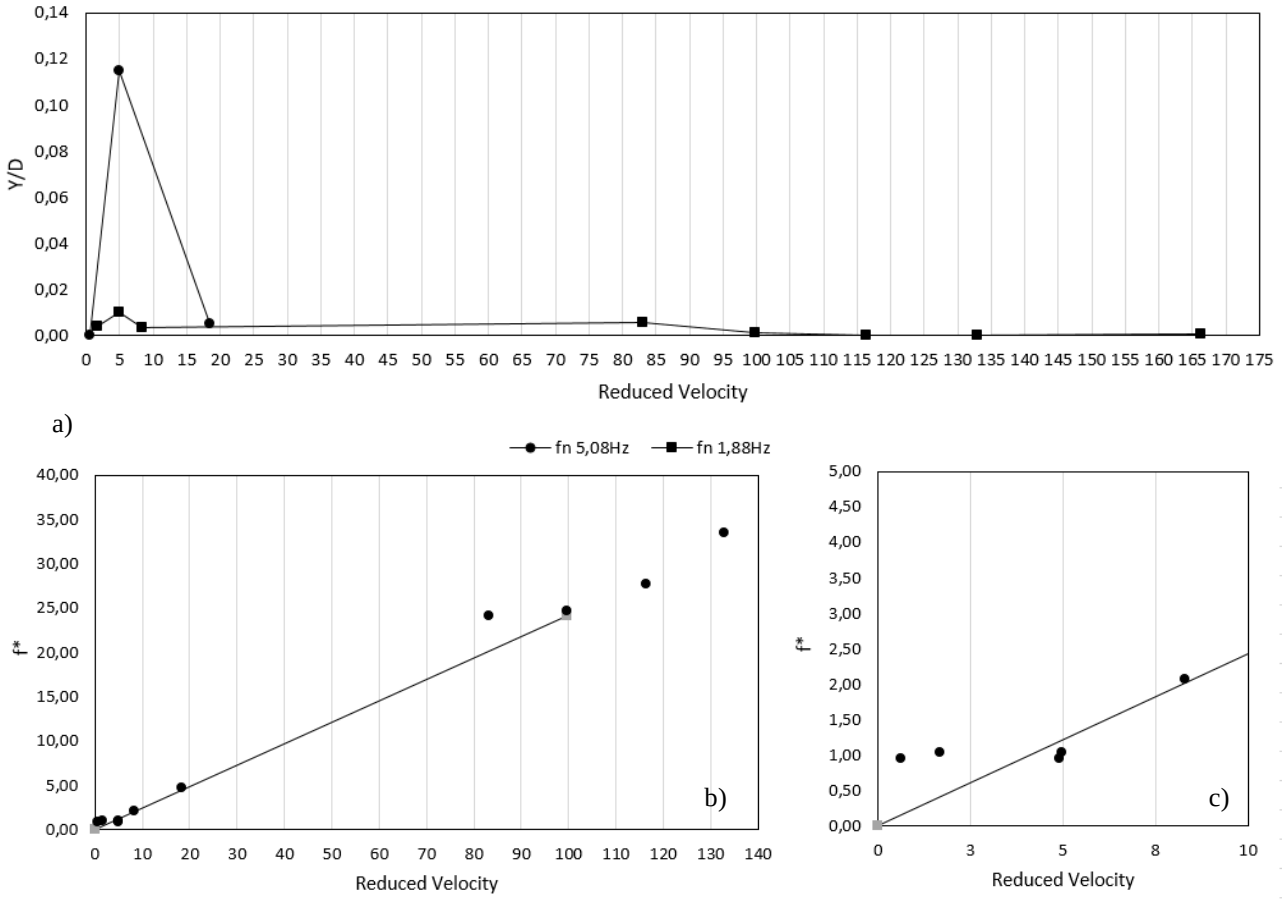

Figure 7. Results of two-dimensional simulations a) Non-dimensional amplitudes, b) frequency ratio and c) detail of frequency ratio in low reduced velocities.

The amplitude of vibration of Case V09, can be observed in Figure 8 a) and shows the vibration behavior for the flow velocity of 8m/s. Initial 4s present a reduction of amplitude as in a free vibration, but after 4s the signal presents an stabilization of behavior with higher amplitudes around $2x10^{-5}$ m. The signal is evaluated applying the frequency power spectrum, Figure 8 b), and the presence of two main frequency peaks are observed. The first one in 2Hz that is related to the theoretical natural frequency, 1.88Hz, and the second peak is in 52Hz and generates a Strouhal number of 0.208, indicating that is the shedding frequency. The power spectrum error stays around 25% in the present cases.

The results of vibration amplitude for the Case V06, with prescribed velocity of 0.5m/s, is presented in Figure 9 a), and the signal characteristics change significantly in comparison with the results from Case V09, Figure 8. In the Case V06, two clear amplitudes and with specific period for each one are observed. This characteristic can indicate that the natural frequency and the shedding frequency are close to synchronize. The amplitude of vibration is also higher in Case V06 than in Case V09. The frequency power spectrum from Case V06 is presented in Figure 9 b) and two

frequency peaks are observed. The first peak is in 2Hz that is linked to the natural frequency and the second one in 4Hz that generates Strouhal number 0.2 and is the shedding vortex frequency. The proximity of the main frequencies shows that synchronization velocity is lower than the one tested.

The results from case V05 are presented in Figure 10 and the amplitude results present a behavior with higher and lower amplitudes, as a beating phenomenon as can be observed in Figure 10 a). The power spectrum presents one frequency peak in 2Hz, with shedding frequency and natural frequency in the same range, but not synchronized.

The results from Case V02 are presented in Figure 11 a) and the increasing values of amplitude are observed. The initial 4s show a beating phenomenon and after that the amplitude keep increasing until reaches the limit of mesh deforming generated in the mesh. The power spectrum in Figure 11 b) shows a peak in 5Hz that can be linked to the natural frequency and vortex shedding. The change in the vortex pattern is the main change observed in Figure 5.

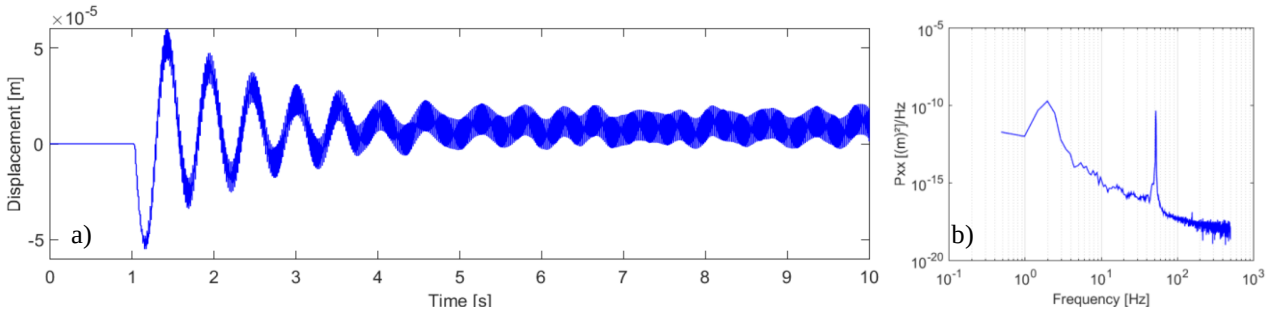

Figure 8. Results for Case V09 – Velocity 8m/s and two-dimensional a) Amplitude response and b) Frequency Power Spectrum.

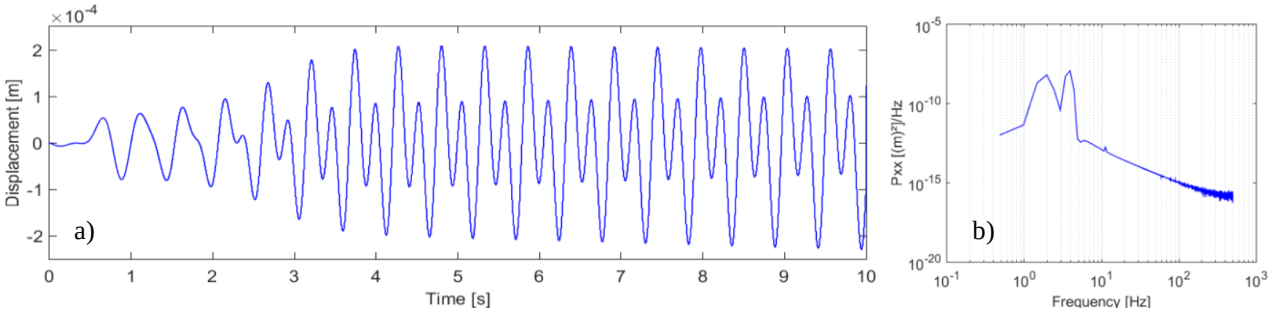

Figure 9. Results for Case V06 – Velocity 0.5m/s and two- dimensional a) Amplitude response and b) Frequency Power Spectrum.

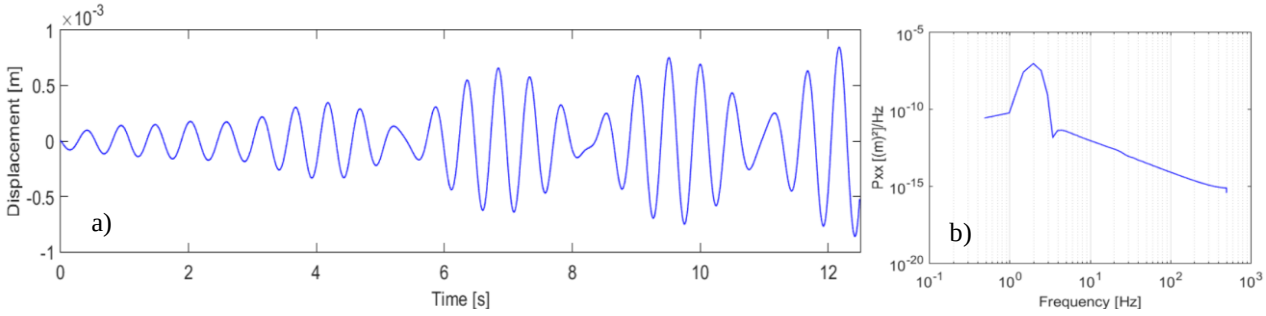

Figure 10. Results for Case V05 – Velocity 0.3m/s and two-dimensional a) Amplitude response and b) Frequency Power Spectrum

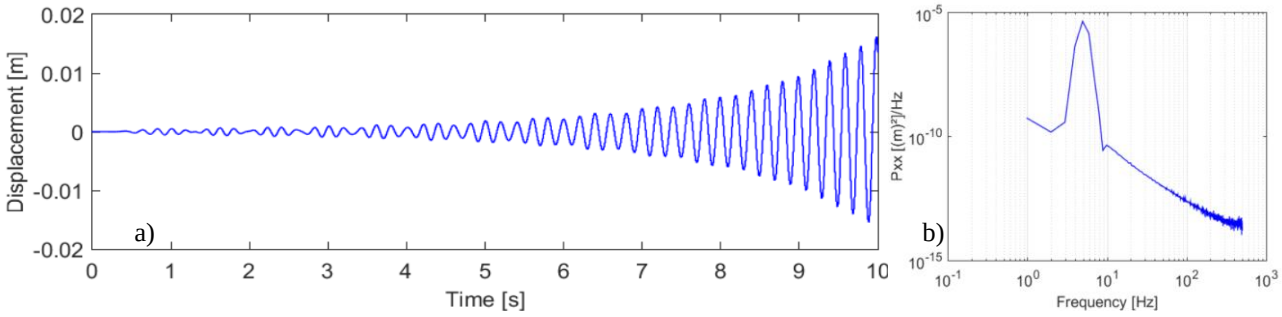

Figure 11. Results for Case V02 – Velocity 0.8m/s and two-dimensional a) Amplitude response and b) Frequency Power Spectrum

3.3 Amplitudes and Frequencie Results – Three-dimensional

The results of three-dimensional analysis for the cases V11 and V12 are presented in Figure 12 and 13. The results in Figure 12 a) are obtained for the flow velocity of 3m/s and the vibration amplitude Y/D = 0.008. The power spectrum presents peaks in 2Hz and 17.8Hz, the first one can be linked to the natural frequency while the second one can be associated with the vortex shedding because generates a Strouhal number of 0.189.

The results with the flow with velocity of 0.2m/s are presented in Figure 13 with lower amplitudes than in Figure 12 a). The power spectrum presents one peak in 2Hz that can be associated with the natural frequency and also with the vortex shedding, but the time history does not present indications of increase in the amplitudes and synchronization.

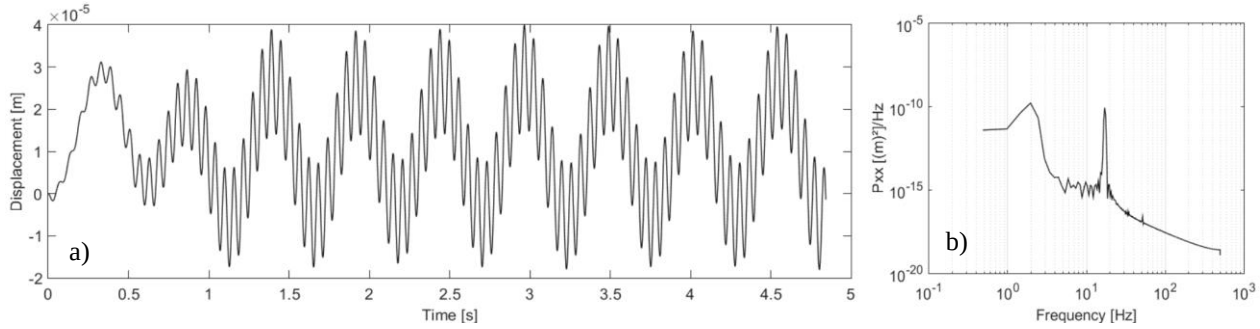

Figure 12 - Results for Case V12 – Velocity 3m/s and three-dimensional a) Amplitude response and b) Frequency Power Spectrum

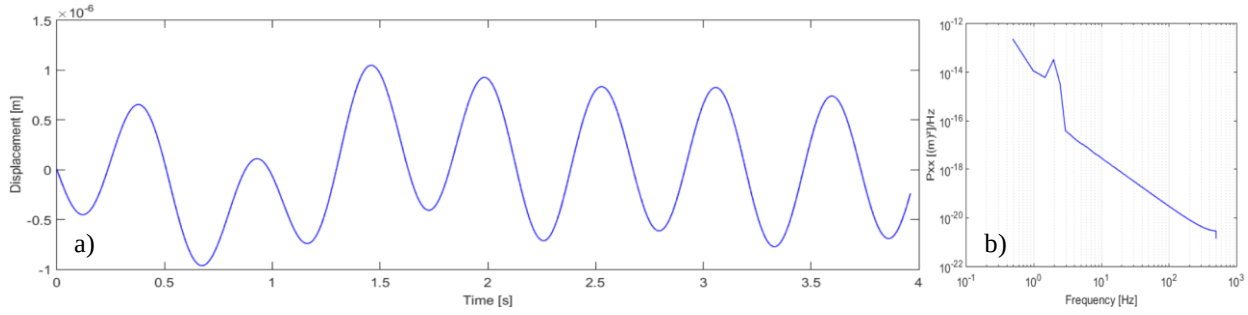

Figure 13- Results for Case V11 – Velocity 0,2m/s and three-dimensional a) Amplitude response and b) Frequency Power Spectrum

4. CONCLUSIONS

The present study showed a numerical analysis comparing fixed cylinders and free to vibrate cylinders to observe vortex shedding patterns. The amplitudes of vibration for a range of reduced velocity was presented with most of results two-dimensional, but two cases three-dimensional.

Fixed and free to vibrate cylinders were analyzed with pressure and velocity fields showing that the cylinder free to vibrate presents an asymmetric pressure field before the cylinder. The velocity field around the cylinder present higher

magnitudes for the fixed cylinder what can be associated with energy of the flow and in the free to vibrate case generates the cylinder movement. The cases free to vibrate and fixed present the vortex pattern with two single vortices in the initial time, but the case V02 shows the change in the pattern of vortex shedding after 7s of simulation, becoming two pairs of vortices and justifying the increase on the vibration amplitude.

The comparison between vibration amplitudes in different reduced velocities showed the beating phenomenon for the velocities close to the natural frequency as observed in case V02 and V05, where the case V02 evolves to the synchronization. The power spectrum presented the natural and vortex shedding frequencies for all the cases, two-dimensional and three-dimensional. Additional analyses are necessary with small changes in the flow velocities, to evaluate the synchronization ranges.

5. REFERENCES

ANSYS Fluent. 2018. Theory Guide.

Blevins, R. D. 1990. *Flow-Induced Vibration*. Segunda Edição. Nova Iorque: Van Nostrand Reinhold.

Dong, S. and Karniadakis, G.E. 2005. DNS of flow past a stationary and oscillatingcylinder at Re = 10 000. *Journal of Fluids and Structures*. v. 20, p. 519–531.

Govardhan, R. and Williamson, C. H. K. 2004. Critical mass in vortex-induced vibration of a cylinder. *European Journal of Mechanics B/ Fluids*. v. 23, p. 17–27.

Gsell, S., Bourguet, R. e Braza, M. 2018. "Three-dimensional flow past a fixed or freely vibrating cylinder in the early turbulent regime". *Physical review fluids* 3, v. 013902.

Jung, S. Y., Kim, J. J., Park, H. W. e Lee, S. J. 2018. "Comparison of flow structures behind rigid and flexible finite cylinders". International Journal of Mechanical Sciences, v.142–143, p. 480–90.

Kelly, S. G. 2000. *Fundamentals of Mechanical Vibrations*. McGraw-Hill, 2ª ed.

Navrose, S. M. 2017. A new regime of multiple states in free vibration of a cylinder at low Re. *Journal of Fluids and Structures*. v. 68, p. 310–321.

Möller, S.V., Silveira, R. S., de Paula, A.V., Indrusiak, M. L. S. e Olinto, C. R. 2015. "Some Features of the Flow on Cylinders in Aerodynamic Channels and Considerations About the Effect of the Blockage Ratio Part 1: Single Cylinder". *ERCOFTAC Bulletin*, v. 104, p. 24-29, 2015.

Roache, P. J. 1994. Perspective: A method for uniform reforming of grid refinement studies. *Jounal of Fluids Engineering*. v. 116, p. 405–413.

Roache, P. J. 1997. Quantification of Uncertainty in Computational Fluid Dynamics. *Annual Review of Fluid Mechanics*. v. 29, p. 123–160.

Tennekes, H., and J. L. Lumley. 1972. *A First Course in Turbulence*. 15° ed. Massachusetts, USA: MIT Press.

Wang, X. K., Wang, C., Li, Y. L. and Tan, S. K. 2017. Flow patterns of a low mass-damping cylinder undergoing vortex-induced vibration: Transition from initial branch an upper branch. *Applied Ocean Research*. v. 62, p. 89–99.

Wilcox, D. C. 2000. *Turbulence Modeling for CFD*. Second Edition. California, EUA: DCW.

Zdravkovich, M. M. *Flow Around Circular Cylinders Vol 1: Fundamentals***.** 1o ed. Vol. 1. New York: Oxford University Press, 1997.

6. RESPONSIBILITY NOTICE

The authors are the only responsible for the printed material included in this paper.